Photovoltaic properties of ammoniated ruthenium oxychloride dye based solar cell

A. FATEHMULLA[*], M. ATIF, W. A. FAROOQ, M. ASLAM, F. YAKUPHANOGLU[a], I. S. YAHIA[b]
Department of Physics and Astronomy, College of Science, King Saud University, P.O.Box 2455, Riyadh-11451, Saudi Arabia
[a]Department of Metallurgical and Materials Engineering, Firat University, Elazig, Turkey
[b]Department of Physics, Faculty of Science, Center of Excellence for Advanced Materials Research, Faculty of Science King Khalid University P.O.Box 9004, Abha, Saudi Arabia

The most promising system for photo-electrochemical cell which has attracted extensively is the mesoporous semiconductor layer based on TiO_2. The micrographs of atomic force microscope have widely supported the nano-structure of TiO_2 thick film on FTO glass. In this study, we have fabricated a dye sensitized solar cell based on nanostructured TiO_2 to investigate the electrical characterization of ammoniated ruthenium oxychloride dye (Ruthenium Red) based solar cell. We used the solar cell with an active area of 0.234 cm^2 to measure a short circuit current density of 53µA/cm^2 and an open circuit voltage of 0.45 V under AM1.5. For the DSSC applications the capacitance-voltage, the conductance-voltage and the series resistance-voltage characteristics of the solar cell were recorded in a wide frequency ranges. The experimental results of the current study led to this conclusion that the photovoltaic performance of the dye-sensitized solar cell can be enhanced/improved by using numerous dyes.

1. Introduction

Due to the increased energy crisis and environment pollution over the past few decades, we have seen a growing concern on the research of photovoltaics. Beside the p-n junction based solar cells the other classes of solar cells which attract considerable interest are dye-sensitized solar cells (DSSCs) and quantum dot sensitized solar cells. The low cost solar cell is dye-sensitized solar cell which was first reported by different investigators like Michael Gratzel and Brian O'Regan at the Ecole ploytechnique Federal de laussanne in 1991 [1-3]. The basic phenomena involved in the development of dye sensitized solar cells are light-activation mechanism similar to the plant photosynthesis. The DSSC are fabricated by depositing a wide band gap semiconductor film over TCO substrate which serves as photo-electrode above which dye molecules are adsorbed. It is found that photo-excited dye electrons move towards the counter electrode (Pt coated TCO) via an external electric circuit to oxidize the electrolyte and hence completing the cycle [1-4]. Keeping in view of Dye-sensitized solar cell advantages like less toxic manufacturing, easy scale-up, light weight, potential use of flexible panels and above all their cost effectiveness over conventional p-n junction devices different investigators are attracted towards its use. The most important component of all the components of a DSSC is a photoelectrode, a kind of nanocrystalline film formed by a wide bandgap semiconductor which plays a very crucial role in the loading of dyes, accepting and transporting

electrons [5, 6]. The following materials such as TiO_2, ZnO, Nb_2O_5, and ZrO_2 [7] can be used as photoelectrodes. The most important among them is TiO_2 due to its advantages of good stability, non-toxicity, low price, etc. [8]. It is observed that the electron transportation in TiO_2 nanocrystalline film is a dynamic process of electron transportation and re-combination influencing directly the photoelectric conversion efficiency of DSSCs. Due to this reason; methods like electron transportation in photoelectrodes and reduction in the charge recombination have been extensively studied by many researchers around the world. Hence there are many techniques or ways to improve electron transportation and reduce their charges recombination in photoelectrodes e.g. by changing the morphology of TiO_2 and decorating the photoelectrodes for example growing compact layers, doping in TiO_2 photoelectrodes etc [9–13]. These techniques or ways can enhance Voc or Jsc to some degree and thus improving the properties of DSSCs. Inspite of photovoltaic parameters, different investigators have tried towards electrical characterization of the DSSCs with ammoniated ruthenium oxychloride dye based solar cell.

In the current study we discussed a method to fabricate dye sensitized solar cell based on nanostructure TiO_2 with ammoniated ruthenium oxychloride dye thus characterizing capacitance-voltage, conductance -voltage, and series resistance - voltage measurements in a wide frequencies ranges.

2. Experimental

2.1. Fabrication of dye-sensitized solar cells

On the FTO glass plate a TiO_2 colloid was positioned using a doctor blading technique. In order to form a thick TiO_2 film about 3–5 µm the process was repeated several times. Finally for sintering the TiO_2 porous film was annealed using a conducting glass sheet at 450 ◦C in air for 30 min. For cooling to 80 ◦C, the TiO_2 film was immersed in ammoniated ruthenium oxychloride dye in absolute ethanol solution for 24 h to absorb the dye completely and then the prepared film was splashed with anhydrous ethanol and dried in moisture-free air. The iodide electrolyte solution consists of 0.5 M lithium iodide mixed with 0.05 M iodine in water-free acetonitrile and it was used for the cell. The active area of the measured solar cells was found to be 0.234 cm^2 approximately. For sputtering over FTO the counter electrode was used in this device and then after dropping the liquid electrolyte above the photoactive TiO_2 electrode, the dye-sensitized solar cell was collected. A Pt-coated FTO electrode was placed over the dye-adsorbed TiO_2 electrode, and the edges of the cell were wrapped with a sealing sheet porous film electrode. The two electrodes were clipped together in the prepared solar cell as shown in Fig. 1.
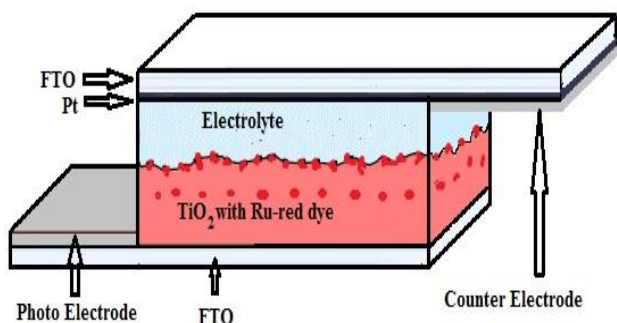

Fig. 1. Schematic of Ammoniated ruthenium oxychloride dye based solar cell.

2.2. Measurments

To carry out the current–voltage characteristics KEITHLEY 4200 semiconductor characterization system was used. In order to perform photovoltaic and light intensity measurements respectively a Small-Area Class-BBA Solar Simulator and TM-206 Solar Power Meter were used. All the measurements were performed at room temperature. Atomic force microscope (AFM) model: Park System, XE100 with a non-contact mode was used to investigate and observe the surface morphology of TiO_2 nanostructured photo-electrode.

3. Results and discussion

3.1. Morphological characteristics

The surface morphology of deposited TiO_2 thick film on FTO was observed by Atomic Force Microscopy. In Fig. 2, the 2D and 3D micrographs of TiO_2/FTO glass of 1×1 µm^2 are shown. The morphology of TiO_2 indicates a nano-structure of grain size approximately 50 nm and roughness 46.78 nm. By using a PARK system XEI software program attached with the AFM system both the grain size and the roughness were determined.
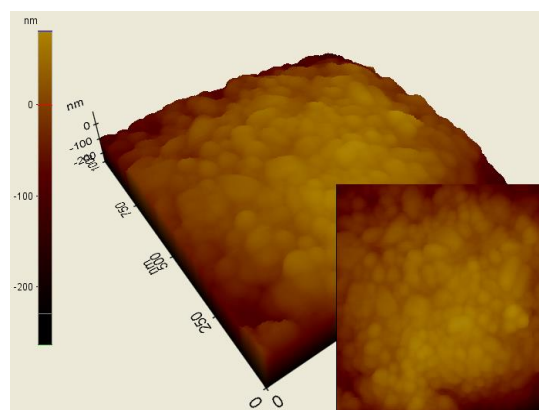

Fig. 2. AFM image of TiO$_2$/FTO glass.

3.2. Photovoltaic properties of FTO/TiO$_2$+Ammoniated ruthenium oxychloride dye based solar cell

Standard solar simulator was used to record the J-V characteristics of the FTO/TiO$_2$+ Ammoniated ruthenium oxychloride dye based solar cell. In Fig. 3 the fourth quadrant of current-voltage characteristics are shown and it can be also observed that the photocurrent and photovoltage values are increasing with the increasing illumination intensities. It can be observed that under 100 mW/ cm^2 illumination the values of short circuit current I_{sc} (53 µA) and open circuit voltage V_{oc} (0.45 V) respectively.
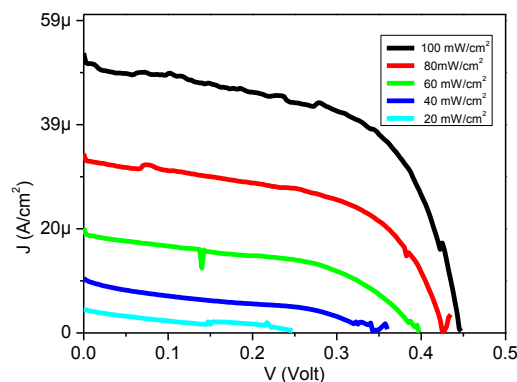

Fig. 3. I-V characteristics of nanostructured TiO$_2$ + Ammoniated ruthenium oxychloride dye based solar cell.

The photovoltaic parameters plots (output power, open circuit voltage, short circuit current) against the incident light intensity were determined which represent the performance of the of sensitized TiO_2 with Ammoniated ruthenium oxychloride dye based solar cell. The experimental results of the electric power are plotted against voltage for TiO_2+ Ammoniated ruthenium oxychloride dye based solar cell which are shown in Fig. 4 about the delivered power to this device.
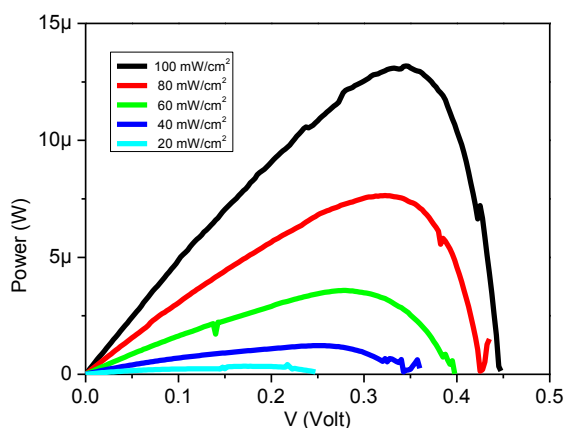

Fig. 4. Output power against voltage curves for nanostructured TiO_2 + Ammoniated ruthenium oxychloride dye based solar cell.

The results of the plots shows an electric power increasing trend with the increasing bias voltage which reaches its maximum power and then start decreasing until reaches zero values if we further increase the applied voltage. The maximum power is calculated by using the formula:

$$P_{max} = I_m \times V_m,\tag{1}$$

In this formula we have observed that I_m is the maximum current and V_m is the maximum voltage at each value of the illumination intensity. Maximum power indicates how much maximum power of the DSSC can be supplied to its external load. The experimental result recorded shows that the maximum power peak is shifted to the higher voltages if we increase incident light as follows: 0.175 V, 0.5 µW at 20 mW/cm^2 and 0.35 V, 13 µW at 100 mW/cm^2. Illumination intensity is plotted against open circuit voltage which is shown in Fig. 5. The illumination dependency of the open circuit voltage clearly demonstrate that V_{oc} shows an increasing trend with the light intensity until it reaches at a saturation value of 0.45 V.
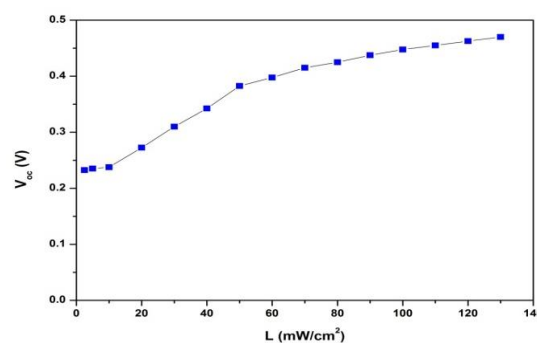

Fig. 5. Illumination dependence of the open circuit voltage V_{oc} for the nanostructured TiO_2+ Ammoniated ruthenium oxychloride dye based solar cell

It is important to mention here that at the lower intensity values the photovoltaic voltage is only proportional to the light intensity [14]. When a sensitizer dye absorbs the incident light it resulted in the generation of a photocurrent in the DSSC and thus causing an ultra-fast electron injection into the conduction band of the TiO_2 [15-18]. Using an arbitrary route method [19] the injected electrons are transported via the network of interconnected oxide particles until they touch the conducting glass substrate.

The oxidized dye is rejuvenated in the electrolyte by fast electron transfer from the iodide ions before it has time to endure irretrievable bleaching [20–22]. Diffusion takes place between the I^{3-} ions formed in the regeneration phase and the short distance to the platinum-coated cathode, where they found to be condensed to create iodide ions to complete the reformative cycle. Both the dye rejuvenation step and the super-sensitization process are identical which is employed in photography to permit the dye molecules in order to vaccinate electrons recurrently without bleaching. From the I-V graphs, under different illuminations, the recorded short circuit currents I_{sc} of the solar cell shows that its increase fulfil linearity with increasing illumination intensity specifically at the higher intensities as shown in Fig.6. This behavior is quite significantly evident from the photo-oxidization and regeneration (by the $I-/I^{3-}$ ions) of the adsorbed dye molecules.
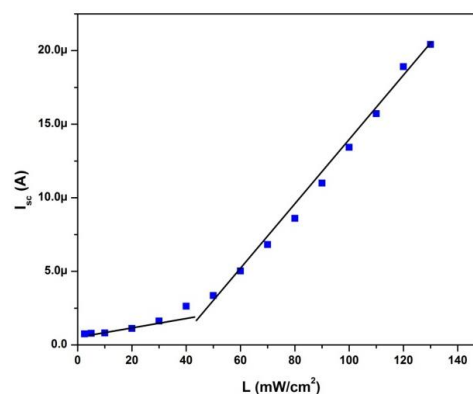

Fig. 6. Light intensity dependence of the short circuit current I_{sc} for the nanostructured TiO_2+ Ammoniated ruthenium oxychloride dye based solar cell.

At both lower and higher radiant powers the short circuit current I_{sc} varies linearly with the power illumination showing that mass transport does not bound to the I_{sc} [23]. The Fig. 7 clearly shows the variation between the short circuit current I_{sc} and open circuit voltage V_{oc}. Hence it is understandable that V_{oc} enhances exponentially with the increase of I_{sc} which mean that the curve plotted clearly demonstrating the variation of V_{oc} with J_{sc} obeying the relation [24-26]:

$$V_{oc} = \frac{nkT}{q} \ln\left(\frac{J_{sc}}{J_o} + 1\right) \qquad (2)$$

Where k is the Boltzmann's constant, n is the diode ideality factor, J_0 is the reverse saturation current density and q is the electric charge. Hence according to Eq. (2), V_{oc} is proportional to the log of I_{sc}. From figure 5 & 6 it is clear that V_{oc} increases with the increase of light intensity [26].
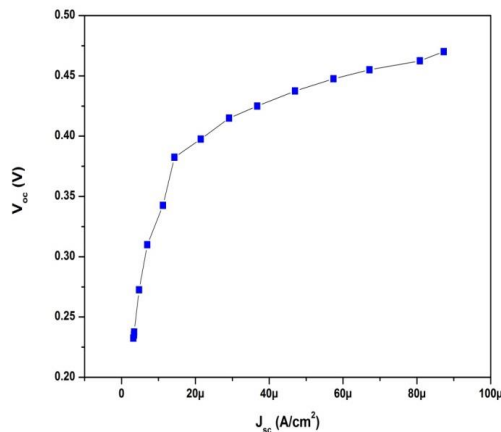

Fig. 7. The plot of short circuit current density J_{sc} as a function of open circuit voltage V_{oc} for the nanostructured TiO$_2$ + Ammoniated ruthenium oxychloride dye based solar cell.

3.3. C-V, G-V and R_s-V characteristics of FTO/TiO$_2$+ Ammoniated ruthenium oxychloride dye based solar cell

Mott-Schottky equation shows a linear relationship between C^{-2}-V [27-29] in a single n-type semiconductor layer for band bending

$$\frac{1}{C_{SC}^2} = \left(\frac{2}{\varepsilon_o N_d e}\right)\left(V - V_{fb} - \frac{kT}{e}\right), \qquad (3)$$

where ε is the dielectric constant of the semiconductor, C_{SC} is the space charge capacitance of semiconductor electrode, ε_0 is the permittivity of the free space, V_{fb} is the flat band potential, V is the applied potential and N_d is the

dopant density. The Mott-Schottky ($1/C^2$ against V) plots of DSSC for TiO$_2$ electrode are shown in Fig. 8(a). This deviation from linearity is in excellent agreement with the results reported by Yin et al. [29] attributing to the recombination effects as well as effect of surface states plus insufficient etching and non-negligible contributions of the Hemholtz layer. Hence Hemholtz layer capacitance can be interpreted as the interface between metallic electrodes and an electrolyte solution that behaves like capacitor which means that it has a capacity of storing electric charge [30].

In Fig. 8(b) the capacitance-voltage characteristics at different frequencies for FTO/TiO$_2$+Ammoniated ruthenium oxychloride dye based solar cell are shown. The experimental results indicate with the increase of the bias voltage from -3.5 V to +3.5 V, the capacitance also shows an increasing trend slowly. Thereafter it reaches its maximum followed by a decrease in its values leading towards saturation with further increase of the bias voltage. Hence by increasing the frequency from 50 kHz to 7 MHz the device capacitance represents a decreasing trend towards zero. Further work is necessary to interpret these results.
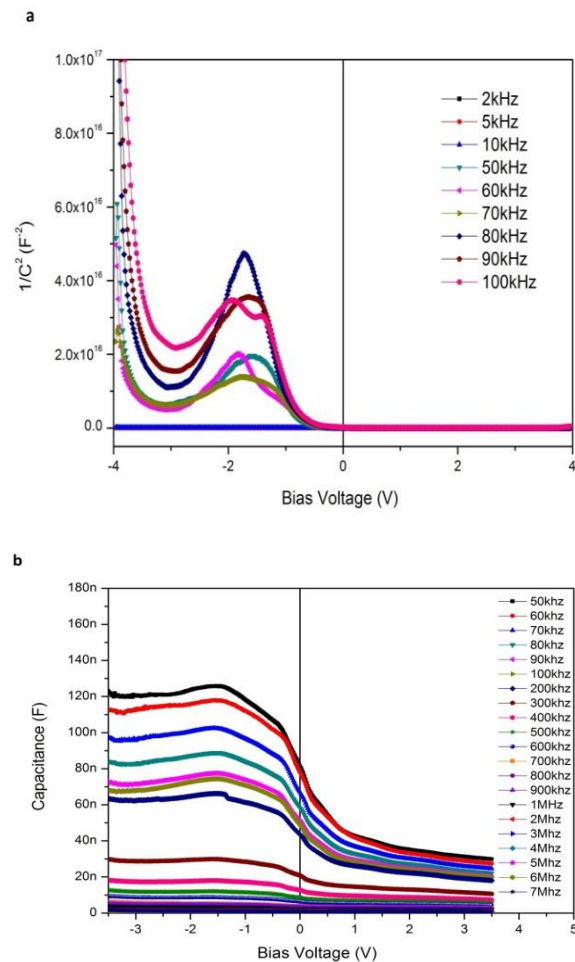
Figs. 8. (a) Mott-Schottky plot of the nanostructured TiO$_2$+ Ammoniated ruthenium oxychloride dye based solar cell at different frequencies. (b) The capacitance profile as a function of biasing voltage at different frequencies for the nanostructured TiO$_2$+ Ammoniated ruthenium oxychloride dye based solar cell.

At different frequencies room temperature Conductance-Voltage (*G-V*) were studied. The plots of conductance against bias voltage at different frequencies are shown in figure 9. When a slight ac signal is applied to the semiconductor device, loss of conductance is observed due to the exchange of majority carriers between interface states and majority carrier band of the semiconductor [31]. The experimental results revealed that conductance is showing a decreasing trend with the increase of applied voltage from -4.0 to +4.0 V. We have also observed the conductance decrease with the increasing applied frequency. This behavior is due to the of capacitance shift towards lower values which mean that there is an increase of the frequency.
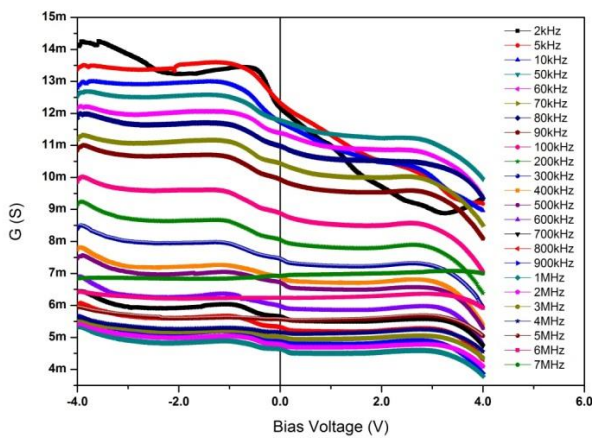

Fig. 9. Conductance-Voltage dependence of the nanostructured TiO$_2$+ Ammoniated ruthenium oxychloride dye based solar cell at different frequencies.
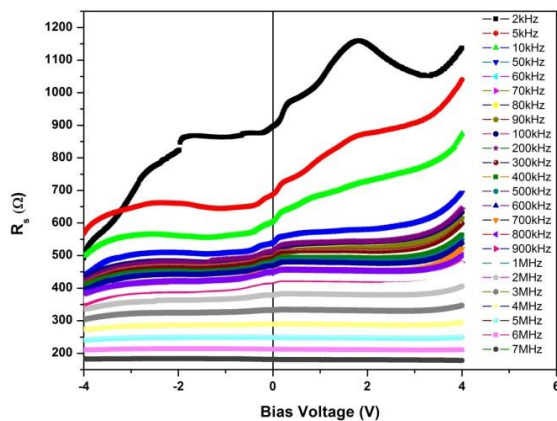

Fig. 10. The plot of series resistance as a function of voltage at different frequencies of the nanostructured TiO$_2$+ Ammoniated ruthenium oxychloride dye based solar cell at different frequencies.

The series resistance dependence of voltage and frequency are shown in Fig. 10. At different frequencies R_s values were measured from cell capacitance C_M and

conductance G_M. Hence for solar cells the following formula holds [32].

$$Y_{MA} = G_{MA} + j\omega C_{MA,} \qquad (4)$$

Hence at different frequencies the series resistance was evaluated by the following relation:

$$R_s = \left(\frac{G_M}{G_{MA}^2 + \omega^2 C_{MA}^2} \right), \qquad (5)$$

The R_s *is the* series resistance which is considered to be a real part of the impedance. At a wide range of frequencies from 2 kHz to 7 MHz, the series resistances were found to be a function of biasing voltage which means that the series resistance is showing an increasing behavior for the bias voltage from -4.0 to +4.0 V if we increase the frequency from 2 kHz to 50 KHz. This resistance increasing trend slows down due to saturation for the frequencies from 60 kHz to 7 MHz. In summary at the lower frequencies, the interface states follow the ac signal and yield an excess capacitance, which is dependent on the frequency [33]. In the case of higher frequencies, the interface states do not follow the ac signal. Hence the contribution due to interface state capacitance in the total capacitance is found to be negligibly small.

4. Conclusion

For the preparation of nano-structure of TiO$_2$ thick film on FTO glass doctor blading technique is used. The experimental results indicate a grain size 50 nm and roughness 46.78 nm of Tio$_2$/FTO glass respectively. In this study the photovoltaic properties (I-V) and impedance spectroscopy (C-V, G-V and R$_s$-V) characteristics of nanostructured TiO$_2$+ Ammoniated ruthenium oxychloride dye based solar cell have been described. The DSSC cell revealed a short circuit current density of 53μA/cm^2 and an open circuit voltage of 0.45 V under AM 1.5 due to the experiment. In order to control the photovoltaic mechanism of the solar cell recombination technique is used. At different frequencies the capacitance–voltage characteristics of the device were compared under negative and positive bias voltages. Due to the experiment the capacitance–voltage characteristics a decreasing trend of capacitance is observed. It is therefore concluded that by improving the optimizing and production conditions a substantial increase in the photoelectrical performance of DSSCs is found.

References

[1] B. O'Regan, M. Gratzel, Nature **353**, 737 (1991).

[2] M. Gratzel, Nature **414**, 338 (2001).

[3] M. Gratzel, Inorg. Chem. **44**, 6841 (2005).

[4] Q. Qin, J. Tao, Y. Yang, Synth. Met. **160**, 1167 (2010).

[5] M. Grätzel, J. Photochem. Photobiol. C **4**, 145 (2003).

[6] J. H. Yum, C. Peter, M. Grätzel, Md. K. Nazeeruddin, Chem Sus Chem **1**, 699 (2008).

[7] R. Jose, T. Velmurugan, R. Seeram, J. Am. Ceram. Soc. **92**, 289 (2009).

[8] A. Hagfeldt, G. Boschloo, L. C. Sun, L. Kloo, H. Pettersson, Chem. Rev. **110**, 6595 (2010).

[9] N. Kopidakis, K. D. Benkstein, J. van de Lagemaat, A. J. Frank, J. Phys. Chem. B **107**, 7759 (2003).

[10] H. Park, W. R. Kim, H. T. Jeong, J. J. Lee, H. G. Kim, W. Y. Choi, Sol. Energy Mater. Sol. Cells **95**, 184 (2011).

[11] S. Lee, J. H. Noh, H. S. Han, D. K. Yim, D. H. Kim, J. K. Lee, J. Y. Kim, H. S. Jung, K. S. Hong, J. Phys. Chem. C **113**, 6878 (2009).

[12] Y. Q. Wang, Y. Z. Hao, H. M. Cheng, J. M. Ma, B. Xu, W. H. Li, S. M. Cai, J. Mater. Sci. **34**, 2773 (1999).

[13] R. Silveyra, L. De La Torre Sáenz, L. Flores, W. Antúnez, V. C. Martínez, A. A. Elguézabal, Catal. Today **107–108**, 602 (2005).

[14] S.-J. Wu, C.-Y. Chen, J.-G. Chen, J.-Y. Li, Y.-L. Tung, K.-C. Ho, C.-G. Wu, Dyes Pigments **84**, 95 (2010).

[15] L. M. Peter, Dye-sensitized nanocrystalline solar cells, Phys. Chem. Chem. Phys. **9**, 2630 (2007).

[16] J. E. Moser, M. Wolf, F. Lenzmann, M. Gratzel, Z. Phys. Chem. **212**, 85 (1999).

[17] B. Burfeindt, C. Zimmermann, S. Ramakrishna, T. Hannappel, B. Meissner, W. Storck, F. Willig, Z. Phys. Chem. **212**, 85 (1999).

[18] Y. Tachibana, J. E. Moser, M. Gratzel, D. R. Klug, J. R. Durrant, J. Phys. Chem. **100**, 20056 (1996).

[19] Y. Wang, J. B. Asbury, T. Lian, J. Phys. Chem. A **104**, 4291 (2000).

[20] J. Nelson, R. E. Chandler, Coord. Chem. Rev. **248**, 1181 (2004).

[21] P. Wang, B. Wenger, R. Humphry-Baker, J. E. Moser, J. Teuscher, W. Kantlehner, J. Mezger, E. V. Stoyanov, S. M. Zakeeruddin, M. Gratzel, J. Am. Chem. Soc. **127**, 6850 (2005).

[22] S. Y. Huang, G. Schlichthorl, A. J. Nozik, M. Gratzel, A. J. Frank, J. Phys. Chem. **B101**, 2576 (1997).

[23] H. Wang, X. Liu, Z. Wang, H. Li, D. Li, Q. Meng, L. Chen, J. Phys. Chem. B **110**, 5970 (2006).

[24] M. L. Rosenblut, N. S. Lewis, J. Phys. Chem. **93**, 3735 (1989).

[25] A. Hagfeldt, H. Lindström, S. Södergren, S.-E. Lindquist, J. Electroanal. Chem. **381**, 39 (1995).

[26] X. Sheng, Y. Zhao, J. Zhai, L. Jiang, D. Zhu, Appl. Phys. A **87**, 715 (2007).

[27] R. C. Kabir-ud-Din, M. A. Owen, Fox, J. Phys. Chem. **85**, 1679 (1981).

[28] J. Bandara, H. C. Weerasinghe, Sol. Energy Mater. Sol. Cells **88**, 341 (2005).

[29] X. Yin, W. Tan, J. Zhang, Y. Weng, X. Xiao, X. Zhou, X. Li, Y. Lin, Colloids Surf. A: Physicochem. Eng. Aspects **326**, 42 (2008).

[30] H. Helmholtz, Pogg. Ann. LXXXIX 211 (1853).

[31] E. H. Nicollian, A. Goetzberger, Appl. Phys. Lett. **7**, 216 (1965).

[32] R. Sahingoz, H. Kanbur, M. Voigt, C. Soykan, Synth. Met. **158**, 727 (2008).

[33] B. Akkal, Z. Benamara, B. Gruzza, L. Bideux, Vacuum **57**, 219 (2000).

_____

[*]Corresponding author: aman@ksu.edu.sa